Scattering of sulfur ions by carbon: Classical-trajectory Monte Carlo results

Katarzyna Słabkowska and Marek Polasik
Institute of Chemistry, Nicholas Copernicus University, Ul. Gagarina 7, 87-100 Toruń, Poland

Maciej Janowicz
Institute of Physics and College of Science, Polish Academy of Sciences, Al. Lotników 32/46, 02-668 Warsaw, Poland
(Received 11 December 2001; revised manuscript received 19 September 2002; published 31 January 2003)

We analyze classically the scattering of sulfur ions by carbon using the classical-trajectory Monte Carlo method. It is assumed that the scatterer and scattered nuclei are coupled to each other as well as to all electrons, but there is no coupling between electrons themselves. To initialize the state of both atoms, quasiexact energies are used that are obtained from the Dirac-Fock method. Effective charges are used to partially take into account the intra-atomic interactions between electrons. We concentrate on the cross sections for production of vacancies in the *K* and *L* shells and capture of electrons to *K*, *L*, and *M* shells of the sulfur ions. The dependence of these cross sections on the energy of the projectile sulfur ions and on the initial charge states of these ions is analyzed. Our results will be helpful in the interpretation of x-ray spectra from highly ionized fast sulfur projectiles passing through a carbon foil.

DOI: 10.1103/PhysRevA.67.012713 PACS number(s): 34.50.Fa, 02.70.Uu

I. INTRODUCTION

It seems to be quite obvious that the knowledge of scattering cross sections for ionization, excitation, and capture processes is of great importance for the interpretation of the x-ray spectra of various elements used as projectiles and target atoms. Theoretical analysis of collisions of heavy atoms is, in general, very difficult because of their inevitably many-body character. There exist a variety of methods to compute the cross sections for collisions of this type. One of them is called the classical-trajectory Monte Carlo (CTMC) method invented in the papers by Abrines and Percival [1–3]. It has been further developed, in particular, by Olson and his groups [4–10] as well as by Cohen [11,12] and others, see, e.g., [13,14]. Interesting modifications of the CTMC have been proposed in [15] and [16] based on the Kirschbaum-Wilets [17] quasiclassical theory of atoms.

Application of classical or quasiclassical methods to the description of atomic scattering requires some justification. The excuse is related to the fact that the full quantum analysis of such many-body processes involving multichannel scattering is still beyond our possibilities even in the nonrelativistic domain. On the other hand, the reliability of the classical description for some regions of characteristic parameters is quite well known since the amazing success of the simple fully classical Gryzinski treatment—see, e.g., [18]—of ionization cross sections of both few- and many-electron atom scattering (the agreement with experiment in the case of capture cross sections is much less impressive, see [19]). The CTMC simulations brought the refinement of approaches of this kind since the many-body interactions and correlations have been explicitly taken into account, at least in part (within the classical physics framework). It is to be noted, however, that every fully classical model of a many-electron atom suffers the instability problems. Even for three electrons in the atom, it is quite difficult to find such initial conditions for the positions and momenta of electrons that the ''autoionization'' due to the collisions of electrons does not take place. For many-electron systems there exist submanifolds of initial conditions such that an electron may escape to infinity in a finite time. The simplest possible way to overcome this difficulty—adopted in this paper—is to neglect the interaction between electrons. More precisely, in the total Hamiltonian of the system consisting of two atoms there are no terms corresponding to interelectron potential energy. However, the initial energies of all electrons are ''exact,'' that is, either taken from experiments or calculated using accurate quantum-chemical methods. The interaction between electrons, while not present in the Hamiltonian, is partially taken into account by ascribing an effective charge to each electron. Simulations based on this idea can be called CTMC with effective charges (CTMC-EC). This is of course a very crude approximation. We have attempted to justify such an effective-charge approach by performing preliminary test simulations for smaller systems, for which both reliable experimental and theoretical quasiclassical results are available. Let us notice in this connection that the authors of [17] proposed a quasiclassical approach which can be used to overcome the instability problem: a momentum-dependent potential is added to the Hamiltonian that enforces the electrons to obey approximately the uncertainty relations and the Pauli exclusion principle. Upon minimization of the Hamiltonian with respect to the location of atomic electrons in the phase space, surprisingly good results can be obtained for the ground-state energies of atoms, comparable to the Hartree-Fock energies [11]. However, the scattering cross sections for light atomic collisions obtained by Cohen in [12] do not seem superior with respect to the standard (i.e., not involving interelectron interactions) CTMC results. On the other hand, the so-called CTMC-EB method (CTMC with energy bounds) developed in that paper seems to be very promising. In an another interesting paper [13], a method to deal with few-electron systems with the help of effective semiempirical central (but not Coulombic) potentials, and an additional three-body potential, has been developed. In this work, how-

TABLE I. Orbital energies of electrons (in a.u.) in the ground state of carbon atom and the ground states of sulfur ions of various charges.

Atom	Charge	Configuration	Orbital	Orbital energy
			$1s$	11.3519
Carbon	0	$1s^2 2s^2 2p_-^2$	$2s$	0.7169
			$2p_-$	0.3897
			$1s$	98.5655
Sulfur	+7	$1s^2 2s^2 2p_-^2 2p^3$	$2s$	14.3732
			$2p_-$	12.2661
			$2p$	12.2481
			$1s$	103.7448
Sulfur	+9	$1s^2 2s^2 2p_-^2 2p^1$	$2s$	17.8934
			$2p_-$	16.2592
			$2p$	16.3108
			$1s$	109.5838
Sulfur	+11	$1s^2 2s^2 2p_-^1$	$2s$	21.7414
			$2p_-$	20.7975
Sulfur	+13	$1s^2 2s^1$	$1s$	115.6061
			$2s$	25.9836
Sulfur	+14	$1s^2$	$1s$	118.5572

ever, we would like to apply the most standard CTMC method to begin with.

One of the peculiarities of the present paper is that we have been interested in ionization of, and charge transfer from, the sulfur ion, which is a projectile. Naturally, we may just change the reference system to consider the sulfur ion as the target. Although the atoms and ions under consideration are already many-electron systems, they can still be dealt with using the nonrelativistic methods. We have checked that the velocities of electrons (even those closest to the nucleus) never become larger than 10% of the velocity of light.

The main body of this work is organized as follows. In Sec. II, we provide a very brief description of the CTMC approach. In Sec. III, we attempt to justify the usefulness of the effective-charge approach to the scattering of few-electron systems by comparing our CTMC-EC results based on effective charges with experimental ones obtained by Shah, Elliott, and Gilbody [20,21] and DuBois [22], and with theoretical ones by Cohen [12]. Section IV is devoted to the presentation of our main results for collision processes involving sulfur ions and carbon atoms.

II. CTMC METHOD

In this section, we summarize the most essential features of the CTMC method following mainly [4], [7], and [11]. This is to make the paper reasonably self-contained. Every CTMC simulation contains three essential steps: (i) choosing the initial conditions, (ii) integration of Hamilton's equations of motion for both nuclei and electrons, and (iii) testing asymptotic trajectories for final states. Regarding step (i), one has to choose six initial values of position and momenta for each electron sampled, in the simplest version of CTMC, from a microcanonical ensemble corresponding to prescribed energies of electrons. In our case, the energy of each electron has been calculated by us using the Dirac-Fock method. All the energies (in atomic units) necessary in our paper are contained in Table I (a "$-$" below the $2p$ subshell symbol indicates that $j=l-\frac{1}{2}$; otherwise $j=l+\frac{1}{2}$).

It is customary in CTMC to use the mean anomaly α, eccentricity e, known from celestial mechanics, and three angular variables ϕ, θ, and ψ, which are the Euler angles, as auxiliary variables to express initial values of positions and momenta. The former quantities are all sampled—separately for each electron—from uniform distribution with $0 \leqslant \alpha < 2\pi$, $0 \leqslant e^2 < 1$, $0 \leqslant \phi \leqslant 2\pi$, $-1 \leqslant \cos\theta \leqslant 1$, and $0 \leqslant \psi \leqslant 2\pi$. With the help of the mean anomaly and eccentricity, we obtain the eccentric angle ξ by solving the equation

$$\alpha = \xi - e \sin\xi. \tag{1}$$

The Kepler equation can be solved just by iteration with satisfactory accuracy. We then obtain the following initial position and momentum of each electron related to its own nucleus:

$$\mathbf{X}^0 = \mathcal{A}(\phi,\theta,\psi)\mathbf{X}_0^0, \tag{2}$$

$$\mathbf{P}^0 = \mathcal{A}(\phi,\theta,\psi)\mathbf{P}_0^0, \tag{3}$$

where

$$\mathbf{X}_0^0 = \begin{pmatrix} 0 \\ [Z_e Z_N/(2U_e)](1-e^2)^{1/2}\sin\xi \\ [Z_e Z_N/(2U_e)](\cos\xi - e) \end{pmatrix}, \tag{4}$$

while $\mathcal{A}(\phi,\theta,\psi)$ is the Euler rotation matrix given by [23]

$$\mathcal{A}=\begin{pmatrix} \cos\phi\cos\theta\cos\psi-\sin\phi\sin\psi & -\cos\phi\cos\theta\sin\psi-\sin\phi\cos\psi & \cos\phi\sin\theta \\ \sin\phi\cos\theta\cos\psi+\cos\psi\sin\psi & -\sin\phi\cos\theta\sin\psi+\cos\phi\cos\psi & \sin\phi\sin\theta \\ -\sin\theta\cos\psi & \sin\theta\sin\psi & \cos\theta \end{pmatrix}. \tag{5}$$

A discussion of other possible conventions for the rotation matrix is discussed, e.g., in [24]. In Eq. (4), U_e denotes the energy of an electron with respect to the nucleus to which it is initially bounded. The variable Z_e is the effective charge of the electron (in a.u.) while Z_N is the charge of the nucleus. Similarly, we have for $\mathbf{P}_0^0$,

$$\mathbf{P}_0^0=\begin{pmatrix} 0 \\ (2mU_e)^{1/2}(1-e^2)^{1/2}\cos\xi/(1-e\cos\xi) \\ -(2mU_e)^{1/2}\sin\xi/(1-e\cos\xi) \end{pmatrix}. \tag{6}$$

To obtain the initial relative motion, we only need to specify the impact parameter b; it is to be sampled from the uniform distribution on the interval $(-b_{\max},b_{\max})$, where $b_{\max}$ is such a value of the collision parameter that the process of interest does not hold for impact parameters larger than $b_{\max}$. The initial values of relative velocities have been taken by us from a related scattering experiment in which x-ray spectra have been measured. It is to be noticed that for every scattering channel, the parameter $b_{\max}$ has had to be different.

The dynamics of the system is governed by the following Hamiltonian function:

$$H=\sum_{i=1}^{2}\frac{\mathbf{P}_i^2}{2M_i}+\sum_{j=1}^{k}\frac{\mathbf{p}_j^2}{2m_e}-\sum_{i=1}^{2}\sum_{j=1}^{k}\frac{Z_{N,i}Z_{e,j}e^2}{|\mathbf{r}_j-\mathbf{R}_i|}+\frac{Z_{N,1}Z_{N,2}e^2}{|\mathbf{R}_1-\mathbf{R}_2|}, \tag{7}$$

where $\mathbf{P}_i$, $i=1,2$ are the momenta of nuclei, M_i, $i=1,2$ are their masses, $\mathbf{p}_j$, $j=1,k$ are the momenta of k electrons, m_e is the electron mass, $\mathbf{R}_i$ and $\mathbf{r}_j$ are positions of nuclei and electrons, respectively, $Z_{N,i}e$ are the charges of nuclei, while $-Z_{e,j}e$ are effective charges of electrons, specified below. In all, we have worked in the reference frame in which one of the nuclei, namely the carbon atom, is at rest at the time $t=0$.

To integrate the Hamilton equations of motion, step (ii), we have used (and compared) several FORTRAN packages obtaining similar (actually, almost identical) results from them. The following algorithms have been used: the Merson algorithm, the Adams-Bashforth-Moulton predictor-corrector, and the Runge-Kutta-Fehlberg fifth-order formula. However, we encounter quite considerable problems here since the time step has had to be extremely small, of the order of 10^{-6} a.u., in order to ensure the full reversibility of the dynamics and satisfactory conservations of the total energy and total angular momentum. This is rather understandable since the electrons in, say, K and L shells of sulfur differ in their energies by one order of magnitude, while the energy of K-shell electrons in carbon is still two orders of magnitude smaller. In connection with it, we plan to use in our further research some specialized algorithms developed to solve N-body problems (cf., e.g., [25,26]) after necessary modifications for the presence of both attraction and repulsion.

In stage (iii), we have had to find whether a particular electron has been ionized, captured, excited, or left without change by the collision process. This has been done by checking the final energy of a given electron with respect to both nuclei as well by checking the final distances between electrons and nuclei (cf. Fig. 1 of [11]).

To each electron we have ascribed an effective charge $Z_{e,i}$ (where the index i labels the electrons) such that the expression $Z_{e,i}Z_N/(2|U_{e,i}|)^{1/2}$ (where $Z_N=Z_{N,\text{sulfur}}$ or $Z_N=Z_{N,\text{carbon}}$, and $U_{e,i}$ has been approximated by an orbital energy from Table I) has given the correct principal quantum number in the one-electron approximation for noninteracting atoms. After the collision process, we have computed the ''classical'' principal quantum numbers according to the formula

$$n_{c,i}=Z_{e,i}Z_N/(|2U_{e,i}|)^{1/2} \tag{8}$$

provided that the electron energy (calculated with respect to a given nucleus) is smaller than zero. In the above equation, $U_{e,i}$ denotes the final binding energy of the ith electron.

With this ''classical'' principal number a quantum number n_i has been associated according to the prescription [7]

$$[(n_i-1)(n_i-\tfrac{1}{2})n_i]^{1/3}\leqslant n_{c,i}\leqslant[(n_i(n_i+\tfrac{1}{2}(n_i+1)]^{1/3}. \tag{9}$$

This quantum number determined the final state of each electron if it had been in a bound state with respect to one of the nuclei.

TABLE II. Cross sections for the single ionization of helium by a proton for various initial energies of the projectile, in units of 10^{-17} cm^2.

Energy (MeV/amu)	Experimental [20]	CTMC-EC	CTMC-KW1	CTMC-KW2	CTMC-EB
0.08	8.32±0.13	6.66±0.20	3.61±0.39	5.50±0.49	7.87±0.73
0.10	8.43±0.18	6.32±0.19	4.15±0.18	5.98±0.5	7.72±0.30
0.20	6.93±0.17	4.01±0.15	4.13±0.36	6.20±0.48	6.91±0.53

TABLE III. Cross sections for the double ionization of helium by a proton for various initial energies of the projectile, in units of 10^{-19} cm^2.

Energy (MeV/amu)	Experimental [20]	CTMC-EC	CTMC-KW1	CTMC-KW2	CTMC-EB
0.08	10.57±1.01	43.84±4.61	3.96±1.72	4.77±1.99	6.07±1.82
0.10	9.61±1.03	28.98±3.48	4.95±1.63	8.80±2.15	7.16±1.97
0.20	5.60±0.17	13.09±2.36	3.30±1.34	12.78±3.04	8.27±2.11

TABLE IV. Cross sections for the process of charge transfer of an electron from the helium atom to a proton, in units of 10^{-17} cm^2.

Energy (MeV/amu)	Experimental [20]	CTMC-EC	CTMC-KW1	CTMC-KW2	CTMC-EB
0.08	4.65±0.23	2.79±0.14	1.85±0.29	2.64±0.35	4.62±0.53
0.10	2.72±0.10	1.29±0.09	1.34±0.11	2.02±0.31	2.80±0.16
0.20	0.365±0.004	0.131±0.024	0.26±0.11	0.18±0.09	0.31±0.11

TABLE V. Single ionization cross sections for the scattering of a fully stripped helium ion by the helium atom, $He+He^{2+}\rightarrow He^{+}+He^{2+}+e$, in units of 10^{-17} cm^2.

Energy (MeV/amu)	Experimental [20]	CTMC-EC	CTMC-KW1	CTMC-KW2	CTMC-EB
0.08	15.25±0.26	11.70±0.47	3.29±1.15	6.53±1.45	19.00±0.87
0.10	18.50±0.21	14.61±0.51	4.94±0.51	8.36±1.16	19.42±1.81
0.20	20.20±0.30	13.63±0.43	8.97±0.45	13.72±0.92	18.13±1.09
0.40	15.14±0.21	7.76±0.29	8.06±0.59	10.88±0.60	12.33±0.45

TABLE VI. Double ionization cross sections for the scattering of a fully stripped helium ion by the helium atom, $He+He^{2+}\rightarrow He^{2+}+He^{2+}+2e$, in units of 10^{-18} cm^2.

Energy (MeV/amu)	Experimental [20]	CTMC-EC	CTMC-KW1	CTMC-KW2	CTMC-EB
0.08	3.66±0.41	16.60±1.40	0.49±0.35	2.72±1.01	0.25±0.25
0.10	5.40±0.34	35.00±2.26	2.97±0.91	4.45±1.14	2.10±0.74
0.20	6.53±0.21	22.98±1.78	6.35±0.91	7.30±0.96	4.90±0.67
0.40	3.11±0.11	5.49±0.67	6.68±0.97	6.49±1.02	4.00±0.48

TABLE VII. Single-capture cross sections for the scattering of a fully stripped helium ion by the helium atom, $He+He^{2+}\rightarrow He^{+}+He^{+}$, in units of 10^{-17} cm^2.

Energy (MeV/amu)	Experimental [20]	CTMC-EC	CTMC-KW1	CTMC-KW2	CTMC-EB
0.08	15.10±0.30	11.06±0.43	16.25±1.15	19.00±1.45	16.03±0.87
0.10	11.50±0.14	6.72±0.33	13.44±1.07	14.35±1.24	10.86±1.31
0.20	2.60±0.02	0.56±0.08	3.34±0.43	3.71±0.52	2.25±0.43
0.40	0.309±0.007	0.056±0.017	0.59±0.17	0.41±0.14	0.22±0.07

TABLE VIII. Cross sections for the ionization-capture reaction in the scattering of a fully stripped helium ion by the helium atom, $He+He^{2+}\rightarrow He^{2+}+He^{+}+e$, in units of 10^{-17} cm^2.

Energy (MeV/amu)	Experimental [20]	CTMC-EC	CTMC-KW1	CTMC-KW2	CTMC-EB
0.08	2.89±0.06	4.81±0.26	1.19±0.17	1.76±0.21	1.72±0.21
0.10	2.36±0.02	3.22±0.21	1.48±0.19	2.05±0.23	1.78±0.21
0.20	0.518±0.005	0.20±0.03	0.70±0.10	0.72±0.10	0.52±0.06
0.40	0.0427±0.0026	0.034±0.024	0.14±0.04	0.14±0.04	0.08±0.02

TABLE IX. Double-capture cross sections for the scattering of a fully stripped helium ion by the helium atom, $He+He^{2+}\rightarrow He^{2+}+He$, in units of 10^{-18} cm^2.

Energy (MeV/amu)	Experimental [22]	CTMC-EC	CTMC-KW1	CTMC-KW2	CTMC-EB
0.08		26.94±1.92	6.43±1.27	7.67±1.55	6.65±1.39
0.10	13.5	9.29±1.06	2.97±0.84	3.46±0.97	6.19±1.33
0.20		0.068±0.048	0.31±0.12	0.31±0.12	0.13±0.08

TABLE X. Cross sections for the single ionization with single-capture reactions in the scattering of a fully stripped helium ion by the lithium atom, $Li+He^{2+}\rightarrow Li^{+}+He^{+}+e$, in units of 10^{-18} cm^2.

Energy (MeV/amu)	Experimental [21]	CTMC-EC
0.075	27.8±4.2	16.02±1.34
0.410	1.22±0.10	0.42±0.17
0.547	0.39±0.13	0.088±0.062

TABLE XI. Single-capture cross sections (no ionization) for the scattering of a fully stripped helium ion by the lithium atom, $Li+He^{2+}\rightarrow Li^{+}+He^{+}$, in units of 10^{-17} cm^2.

Energy (MeV/amu)	Experimental [21]	CTMC-EC
0.075	9.39±0.62	8.18±0.40
0.410	5.86±0.42	2.14±0.41
0.547	0.225±0.014	0.0484±0.0144

TABLE XII. Double ionization cross sections for the scattering of a fully stripped helium ion by the lithium atom, $Li+He^{2+}\rightarrow Li^{2+}+He^{2+}+2e$, in units of 10^{-18} cm^2.

Energy (MeV/amu)	Experimental [21]	CTMC-EC
0.410	3.95±0.20	3.80±0.53
0.547	2.88±0.24	2.55±0.47

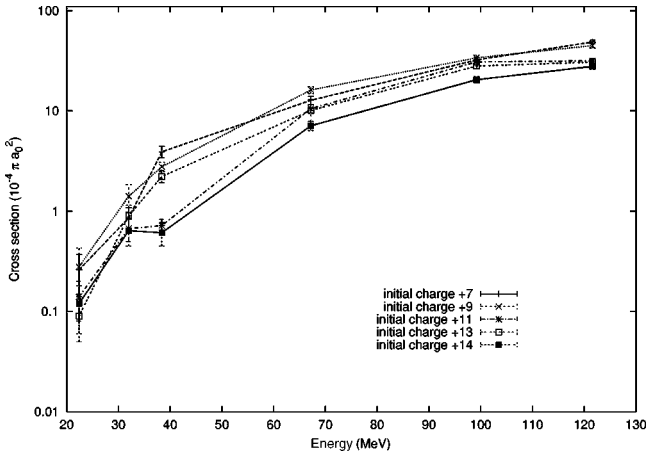

FIG. 1. Cross sections for the ionization of the K shell of the sulfur ion with initial charges $+7$, $+9$, $+11$, $+13$, and $+14$, for various initial energies of the projectile, in units of $10^{-4}\pi a_0^2$. $10^{-4}\pi a_0^2=0.879\,735\times10^{-20}$ cm^2.

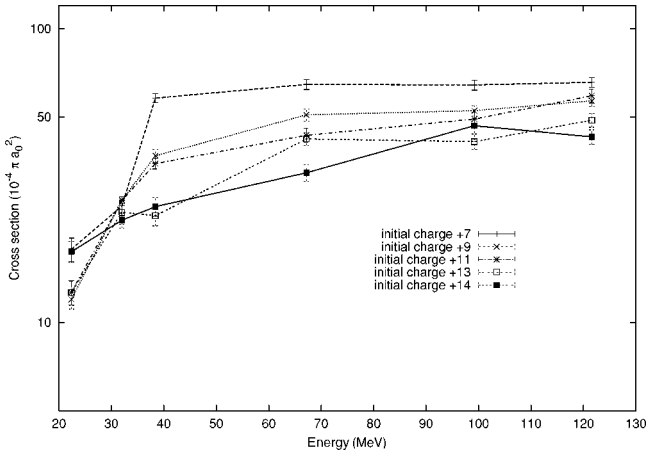

FIG. 2. Cross sections for the electron transition from the K to L shell of the sulfur ions for various initial charges and various initial energies of the projectile, in units of $10^{-4}\pi a_0^2$.

The cross section σ_O for a process O, where O is either vacancy or capture, is given in CTMC by the expression

$$\sigma_O = \frac{N_O}{N_{\text{tot}}} \pi b_{\max}^2, \tag{10}$$

where N_O is the number of times the process O occurred and N_{tot} is the total number of trajectories run. The statistical error $\delta\sigma_O$ is given by

$$\delta\sigma_O = \sigma_O \sqrt{\frac{N_{\text{tot}} - N_O}{N_O N_{\text{tot}}}}. \tag{11}$$

III. CTMC-EC, QUASICLASSICAL SIMULATIONS, AND EXPERIMENTAL RESULTS FOR SCATTERING OF FEW-ELECTRON SYSTEMS

We have performed some preliminary simulations to compare the simple-man approach (CTMC-EC) based on ascribing an effective charge to each electron with quasiclassical ones based on the Kirschbaum-Wilets effective Hamiltonian, which partially takes into account the uncertainty principle and exclusion principle as well as with Cohen's CTMC-EB simulations, in which the dynamics of every electron are constrained by a specially chosen potential which guarantees that the electron energy cannot be too small (hence the ''autoionization'' cannot happen). For each entry in the following tables we have performed simulations using 5000 trajectories. In Table II, we show the cross sections for single ionization of a helium atom by protons for several energies of the projectile.

The latter three columns in Table II refer to three groups of results obtained by Cohen using two variants of the Kirschbaum-Wilets approach and Cohen's own CTMC with energy constraints (cf. [12] for the details). Table III contains cross sections for the double ionization of helium by a proton for several initial velocities of the projectile.

In Table IV, we provide the comparison of experimental and various theoretical results for the single-electron charge transfer from helium to proton.

As a further check of performance of the effective-charge approach, we have also simulated the scattering of an α particle by helium atoms. Tables V–IX contain comparison of various theoretical and experimental results for single and double ionization, single and double electron capture, as well as the ionization-capture reaction.

Let us notice that the processes for which the cross sections are described in Tables V and VIII are different: the first one consists in the single ionization of a helium atom by the α particle. In the second process, we have the capture of one electron from the helium atom by the α particle with the accompanying ionization of the second electron. Thus, in the first process one electron remains with the target atom, in the second process it is the projectile which has one electron more, while the target atom is fully stripped after the collision.

Tables X–XII contain several cross sections for some reactions in the scattering of α particles by lithium, for which we do not know the CTMC-KW or CTMC-EB results, so that only the experimental and our CTMC-EC results are given.

From the above tables, one might conclude that the agreement of existing classical or quasiclassical and experimental results in the scattering of light atoms cannot be called very good. However, the former give at least a good estimate of the orders of magnitude, and provide a correct qualitative picture of how the cross sections change with the energy of projectiles. What is somewhat surprising about the above results is that the Kirschbaum-Wilets quasiclassical simulations do not offer any systematic improvement over the effective-charge approach which completely neglects both interelectron interactions and the quantum-mechanical uncertainty and exclusion principles—such an improvement is visible only for very large energies of the projectile. On the contrary, we can see in the above tables that the effective-charge simulations can sometimes provide better results (i.e., closer to experimental ones) than the Kirschbaum-Wilets simulations. The advantage of the latter is conceptual rather than practical; by that we mean that they form one of the first attempts to go beyond the simplest formulations of CTMC in scattering processes, including all the interactions and some quantum features. It seems to us that the above tables provide justification to our belief that ignoring the interelectron interactions (or taking them into account only via constant effective charges) does not lead to catastrophic consequences. However, the procedures applied here can only be considered as a first step toward reliable semiclassical simulations of complicated multielectron systems, and our results need to be viewed with considerable skepticism, especially for large velocities of the projectiles. Let us finally mention that a simple approach with effective charges ascribed to every electron has been recently advocated by Berakdar [27] in his work devoted to an approximate solution to the many-particle Schrödinger equation.

IV. RESULTS AND DISCUSSION

We have obtained the cross sections for six different energies of the projectile (22.4 MeV, 32.0 MeV, 38.4 MeV, 67.2 MeV, 99.2 MeV, and 121.6 MeV) corresponding to experimental conditions of scattering of sulfur ions on the carbon foils [28,29]. The incident sulfur ions in these experiments have had the initial charge $+7$, $+13$ and $+14$ electron charges. To obtain more representative picture of the underlying processes we have performed our simulations additionally for the ion charges $+9$ and $+11$. All sulfur ions with the above charges have their electrons in either K or L shells, so that only for these shells is the cross section for vacancy (appearance of hole) meaningful. The vacancies in K and L shells can appear due to ionization of a sulfur ion or excitation of this ion, or, finally, due to the capture of an electron by the carbon atom. Let us notice that in our classical procedure we could track processes which are not distinguishable from the quantum-mechanical point of view. This means that, since classical particles are distinguishable, we could follow the motion, and establish the final state, of every individual electron.

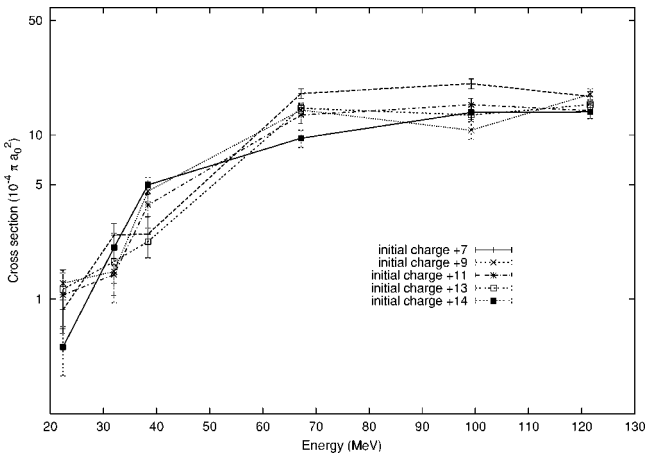

FIG. 3. Cross sections for the electron transition from the K shell to higher-than-L shells for various initial charges and various initial energies of the projectile, in units of $10^{-4}\pi a_0^2$.

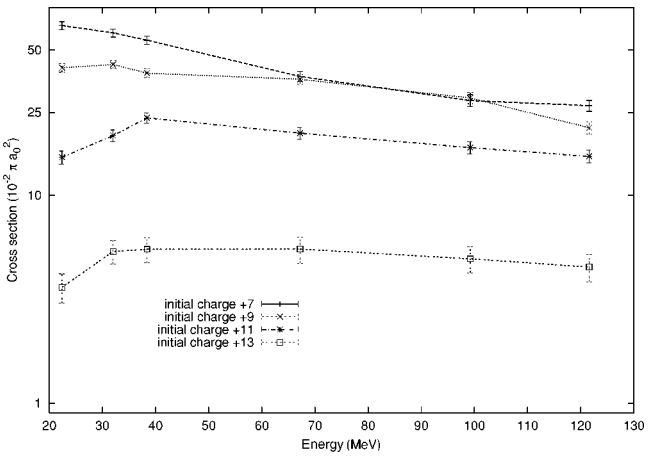

FIG. 5. Cross sections for the ionization of the L shell of the sulfur ions for various initial charges and various initial energies of the projectile, in units of $10^{-2}\pi a_0^2$.

A. Cross sections for transitions from the K shell

In Figs. 1–4, we have placed our results for the cross sections corresponding to the processes of ionization and excitation for the K electrons of a sulfur ion. The key inside each figure refers to the points and vertical lines associated with the corresponding error bars. The lines which join the points do not have any independent meaning.

Each entry in the above figures is a result of sampling of 6000 simulations. It is to be noted that for low initial energy of the projectile (up to 38.4 MeV) the transition probabilities for all processes involving K electrons are small, or very small. Indeed, the cross sections for ionization, and for transitions to higher-than-L shells up to the energy 38.4 MeV, are, at best, only of qualitative value, since there have been only very few transitions and the statistical errors are of the same order as the values themselves. Nevertheless, we can observe quite pronounced trends in changes of cross sections with the initial energy of the projectile. As one might expect, the cross sections grow with this energy. For too small velocity of the projectile, the transfer of energy to the K electrons is insufficient to cause any remarkable change in their state, except of the transfer to the carbon atom; even the cross sections for the K-to-L excitation are small. It is to be observed that the cross section for the capture to the carbon atom is larger than any other cross sections related to K electrons for all energies of the projectile we investigated. But the transition probabilities even for this process never exceeded 0.25 for any impact parameter. Also, we observe that while the ionization (and, to a lesser extent, the excitation cross sections) grow quite rapidly with the projectile energy, the electron-transfer cross section exhibits the tendency to saturate and even starts to decrease for very large velocities, remaining, however, the largest of all cross sections. This behavior is to be expected from the general characteristics of scattering processes in ''small'' and ''intermediate'' regions of the projectile energy, cf. [30]. Of course, the projectile energies involved here are small or intermediate only in relation to the large binding energy of the K-shell sulfur electrons. We also infer from the above figures that with increasing initial charge of the sulfur ions the cross

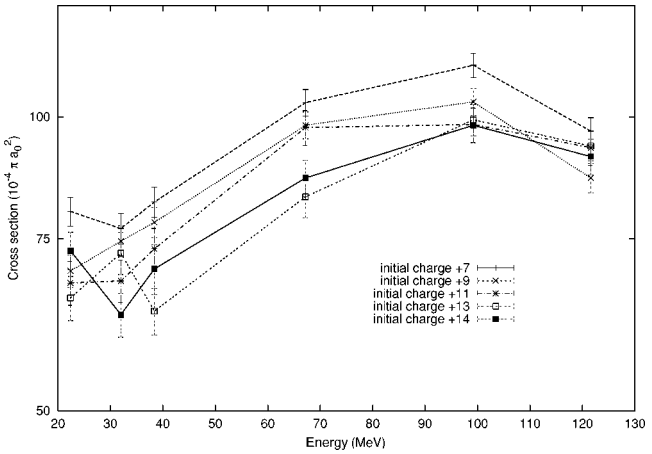

FIG. 4. Cross sections for the electron capture from the K shell of the sulfur ion to the carbon atom for various initial charges of and various initial energies of the projectile, in units of $10^{-4}\pi a_0^2$.

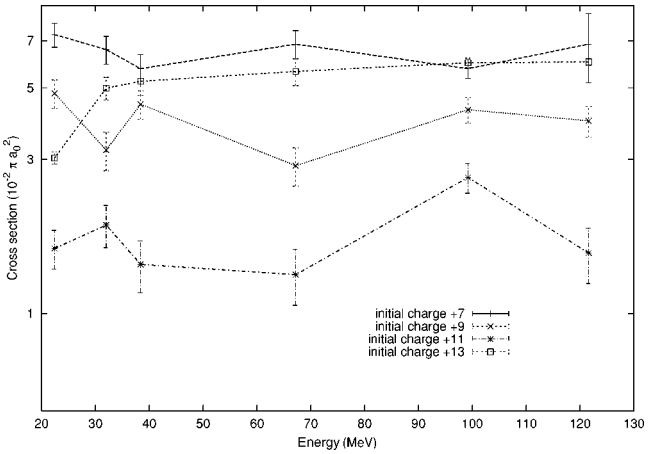

FIG. 6. Cross sections for the electron transition from L shell to K shell of the sulfur ions for various initial charges and various initial energies of the projectile, in units of $10^{-2}\pi a_0^2$.

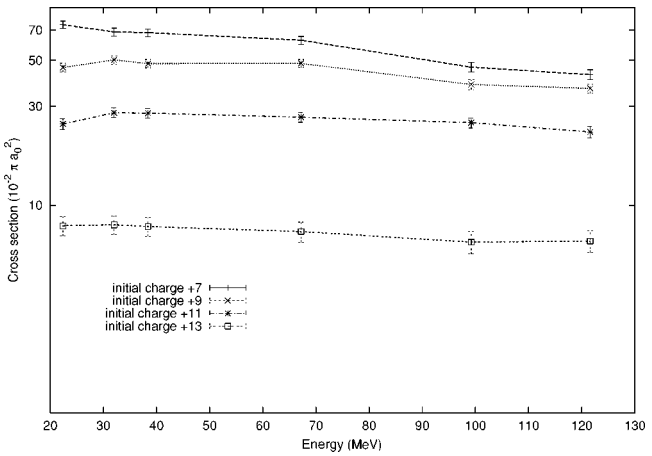

FIG. 7. Cross sections for the electron transition from L shell to M shell of the sulfur ions for various initial charges and various initial energies of the projectile, in units of $10^{-2}\pi a_0^2$.

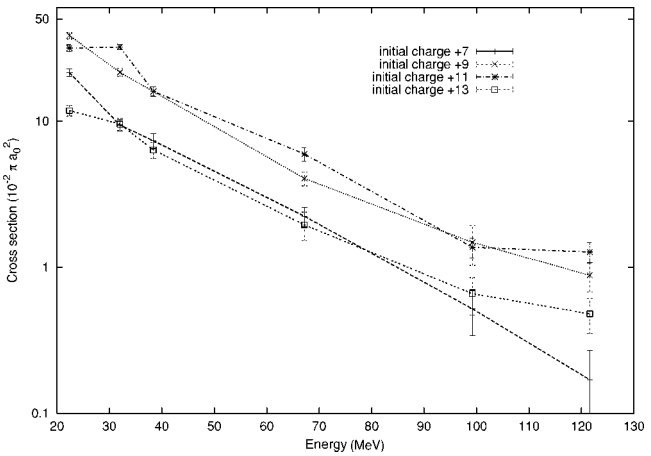

FIG. 9. Cross sections for the electron transfer from the L shell of the sulfur ion to the carbon atom for various initial charges and energies of the projectile, in units of $10^{-2}\pi a_0^2$.

sections generally decrease, which, again, is a consequence of the growing binding energy of electrons in the shell closest to the nucleus.

B. Cross sections for the transitions from the L shell

The most obvious observation about the cross sections for processes involving L electrons is that for low initial energy of the projectile (up to 38.4 MeV) they are, in general, considerably larger than those for the K shell. This is natural because the binding energy of K electrons is about five times greater than L electrons. The results of simulations are presented in Figs. 5–9, where, again, the key inside each figure refers to the points and error bars, while the lines joining points have no meaning by themselves.

The dependence of processes producing vacancies in the L shell on the projectile energy has a maximum. The location of this maximum changes with the change of the initial charge state of the ion and moves toward the higher velocities of the projectile with growing initial charge. This is reasonable because the binding energy of L electrons grows with larger ionization degree. For larger ionization degree, the cross section for the vacancy in the L shell becomes smaller. This effect is, on the one hand, due to the smaller number of electrons in the L shell, and, on the other hand, due to the growing binding energy. We have to notice that our results for the transition from the L to K shell are again of only a qualitative nature since the transition probabilities are again small. On the other hand, the contributions of transitions from L to higher-than-M shells to the vacancy production are non-negligible, and even comparable to the contributions of the ionization process. It is also interesting that the cross section for excitation from L to M shells seems to dominate over the ionization cross section. Moreover, the cross section for the electron transfer from the L shell of the sulfur ion to the carbon atom, shown in Fig. 9, decreases with the projectile velocity much more rapidly than the ionization or excitation cross section, which is a rather typical behavior for such collisions.

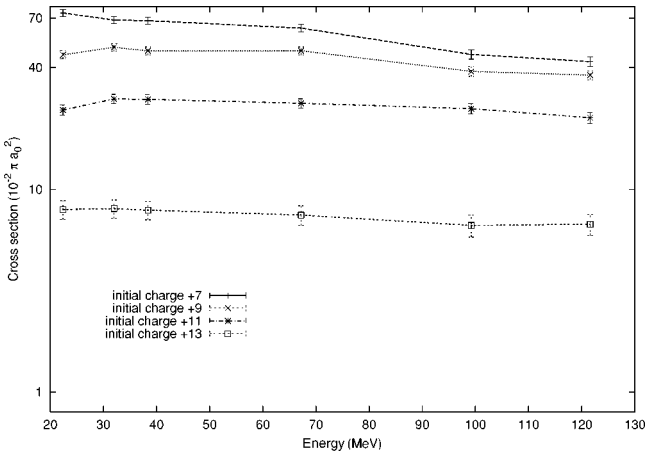

FIG. 8. Cross sections for the electron transition from the L shell to all higher-than-M shells of the sulfur ions for various initial charges and various initial energies of the projectile, in units of $10^{-2}\pi a_0^2$.

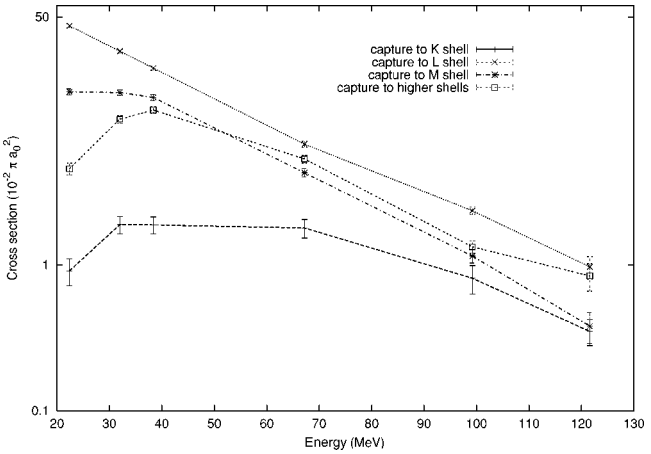

FIG. 10. Cross sections for the electron transfer from the carbon atom to K, L, M, and higher (H) shells of the sulfur ion for various initial energies of the projectile, in units of $10^{-2}\pi a_0^2$.

TABLE XIII. Cross sections for the excessive, unphysical population of the K shell of a sulfur ion with initially two electrons on the K shell (initial charge $+14$) after the collision with the carbon atom for four initial energies of the projectile, in units of $10^{-2}\pi a_0^2$.

Energy (MeV)			
38.4	67.2	99.2	121.6
1.12 ± 0.09	0.98 ± 0.09	0.34 ± 0.05	0.16 ± 0.04

C. Cross sections for the electron capture

We have also tracked the process of charge transfer from the target-carbon atom to the sulfur projectile. Let us notice that we have not recorded any contribution to such transfer from the carbon electrons of the L shell. On the other hand, the transfer from the K-shell electrons of carbon has been quite considerable (see Fig. 10).

Figure 10 shows the results for the electron capture to K, L, M, and higher (H) shells of the sulfur ion. The cross section for the capture to the K shell is very small and has been obtained from just several ''successful'' trajectories of the total number of 6000. The cross sections for the transfer to shells higher than M of the sulfur ion seem to have a maximum in the region of the projectile energies we consider; on the other hand, the cross sections for the capture to L and M shells, being much larger for the lowest velocity, decrease monotonically and rapidly. One can observe that the kinetic energy of electrons corresponding to the relative motion with the projectile energy 22.4 MeV is approximately equal to 14.0 a.u., which is very close to the binding energies of L-shell sulfur electrons, especially for the sulfur ion charge $Q=+7$, as well as of K-shell carbon electrons; hence the transfer cross section involving these two shells should be very large, which is indeed the case.

As mentioned above, the simplest method of simulation of collisional processes employed here is not without serious shortcomings. As a result of the purely classical treatment of electrons with no account of interelectron interactions, the correct shell structure is not preserved in the final state. This means that, in particular, we can and do have more than two electrons in the K shell. In Table XIII, we provide some ''cross sections'' for the unphysical process of having finally three electrons on the K shell of a sulfur ion, which had initially two electrons on this shell, for initial charge $+14$ and four projectile energies.

In spite of those quite considerable cross sections for unphysical processes, we still believe that our results for ionization, excitation, and capture reported above still possess at least qualitative value. It is to be stressed, however, that the ''simple-man'' simulations performed by us should and will be followed by a more refined approach, in which pathological effects do not appear.

V. CONCLUDING REMARKS

In this paper, the classical-trajectory Monte Carlo simulations are presented leading to the determination of cross sections for vacancy in, and electron capture to, the inner-shell electrons of the projectiles which were the sulfur ions. The dependence of these cross sections on the energy of the projectile sulfur ions as well as on the initial charge states of these ions is analyzed. It has been found that for low initial energy of the projectile, the processes involving the L shell are dominant in the scattering: the cross sections for all processes creating a vacancy (hole) in the L shell are much larger than those for the case of the K shell; on the other hand, the cross section for the capture to the L shell are, in the generic case, again larger than those for the other shells. The cross sections for the hole production in the K shell of the sulfur ions are very small for low initial energy of the projectile, while the cross sections for the capture to this shell are almost negligible due to the large binding energies of electrons in this shell. However, the ionization of the K shell of the sulfur ions and, to a lesser extent, the K-to-L-shell excitation cross sections grow quite rapidly with the projectile energy.

The cross sections have been obtained here with the help of the most standard CTMC, which does not involve the electron-electron interactions but ascribes a particular effective charge to each electron of both the target and projectile atoms. The natural next step would be to employ the refinements of this technique developed by Olson and Cohen (i.e., the Kirschbaum-Wilets CTMC and CTMC with energy bounds) and compare them with the results of the ''standard'' approach. We want to perform such simulations using more efficient and more reliable numerical algorithms connected with the Kustaanheimo-Stiefel regularization of the Kepler problem [25,26,31]. Let us notice that the simulations presented here have been laborious since, in particular, essentially each entry in the tables shown above required first the determination of a separate value of the maximal impact factor.

There are two other important issues to be addressed in the future. One may argue that the electrons in the simulations should initially have not only correct energies, but also correct quantum-mechanical values of other observables, in particular those of the angular momentum. Indeed, it seems that classical theory makes better predictions of the cross sections for ionization of hydrogen atoms by protons if the electron is assumed to have a low (almost zero) angular momentum. The eccentric anomaly e in such refined simulations would be sampled not from a uniform probability distribution, but rather uniquely defined by the energy and angular momentum. In a somewhat relaxed version, the above requirement leads to the ''correct'' angular momenta within the independent-particle model. But then it would also be necessary to take (somehow) into account a ''classical spin'' of an electron, since for small angular momenta the electron passes very close to the nucleus and the coupling of the magnetic moment of the electron with the magnetic field of the nucleus (which moves fast in the reference frame associated with the electron) is by no means negligible. We hope to address these important points in future publications.

ACKNOWLEDGMENT

This work was supported by the Polish Committee for Scientific Research (KBN), Grant No. 2P03B 019 16.

[1] R. Abrines and I.C. Percival, Phys. Lett. **13**, 216 (1964).
[2] R. Abrines and I.C. Percival, Proc. Phys. Soc. London, **88**, 861 (1966).
[3] R. Abrines and I.C. Percival, Proc. Phys. Soc. London, **88**, 873 (1966).
[4] R.E. Olson and A. Salop, Phys. Rev. A **16**, 531 (1977).
[5] K.H. Berkner, W.G. Graham, R.V. Pyle, A.S. Schlachter, J.W. Stearns, and R.E. Olson, J. Phys. B **11**, 875 (1978).
[6] A. Müller, B. Schuch, W. Groh, E. Salzborn, H.F. Beyer, P.H. Mokler, and R.E. Olson, Phys. Rev. A **33**, 3010 (1986).
[7] R.E. Olson, J. Ullrich, and H. Schmidt-Böcking, Phys. Rev. A **39**, 5572 (1989).
[8] A. Gensmantel, J. Ullrich, R. Dörner, R.E. Olson, K. Ullmann, E. Forberich, S. Lencinas, and H. Schmidt-Böcking, Phys. Rev. A **45**, 4572 (1992).
[9] C.J. Wood, C.R. Feeler, and R.E. Olson, Phys. Rev. A **56**, 3701 (1997).
[10] M.L. McKenzie and R.E. Olson, Phys. Rev. A **35**, 2863 (1987).
[11] J.S. Cohen, Phys. Rev. A **27**, 167 (1983).
[12] J.S. Cohen, Phys. Rev. A **36**, 2024 (1987).
[13] G. Peach, S.L. Willis, and M.R.C. McDowell, J. Phys. B **18**, 3921 (1985).
[14] G. Bandarage and R. Parson, Phys. Rev. A **41**, 5878 (1990).
[15] D. Zajfman and D. Maor, Phys. Rev. Lett. **56**, 320 (1986).
[16] J.S. Cohen, Phys. Rev. A **54**, 573 (1996).
[17] C.L. Kirschbaum and L. Wilets, Phys. Rev. A **21**, 834 (1980).
[18] M. Gryziński, Phys. Rev. **138**, A336 (1965).
[19] J.D. Garcia, E. Guerjoy, and J.E. Welker, Phys. Rev. **165**, 72 (1968).
[20] M.B. Shah and H.B. Gilbody, J. Phys. B **18**, 899 (1985).
[21] M.B. Shah, D.S. Elliott, and H.B. Gilbody, J. Phys. B **18**, 4245 (1985).
[22] R.D. DuBois, Phys. Rev. A **36**, 2585 (1987).
[23] B.G. Wybourne, *Classical Groups for Physicists* (Wiley, New York, 1974).
[24] H. Goldstein, C. Poole, and J. Safko, *Classical Mechanics* (Addison-Wesley, San Francisco, 2002).
[25] S.J. Aarseth, in *Multiple Time Scales*, edited by J.U. Brackbill and N.I. Cohen (Academic Press, New York, 1985).
[26] Y. Funato, P. Hut, S. McMillan, and J. Makino, Astron. J. **112**, 1697 (1996).
[27] J. Berakdar, Phys. Rev. A **55**, 1994 (1997).
[28] U. Majewska, K. Słabkowska, M. Polasik, J. Braziewicz, D. Banaś, T. Czyżewski, I. Fijał, M. Jaskóał, A. Korman, and S. Chojnacki, J. Phys. B **35**, 1941 (2002).
[29] J. Braziewicz, U. Majewska, K. Słabkowska, M. Polasik, I. Fijał, M. Jaskóła, A. Korman, W. Czarnacki, S. Chojnacki, and W. Kretschmer, J. Phys. B (to be published).
[30] B.H. Bransden and M.R.C. McDowell, *Charge Exchange and the Theory of Ion-Atom Collisions* (Clarendon Press, Oxford, 1992).
[31] P. Kustaanheimo and E. Stiefel, J. Reine Angew. Math. **218**, 204 (1965).